Electronic Supplementary Material (ESI) for Physical Chemistry Chemical Physics.

Electronic Supplementary Information: Complexation and organization of Doxorubicin on polystyrene sulfonate chains: impact on Doxorubicin dimerization and quenching

Natalie Solfrid Gjerde[a], Alessandro Nicola Nardi[a], Cheng Giuseppe Chen[a], Paolo di Gianvincenzo[b], Marco D'Abramo[a], Anita Scipioni[a], Luciano Galantini[a], Mauro Giustini*[a], and Sergio E. Moya†[a,b]

[a]Chemistry Department, "La Sapienza" University of Rome, P. le A. Moro 5, Roma, 00185, Italy

[b]Center for Cooperative Research in Biomaterials (CIC biomaGUNE), Basque Research and Technology Alliance (BRTA), Paseo Miramon 182 C, 20014 Donostia-San Sebastian, Spain

*mauro.giustini@uniroma1.it

†smoya@cicbiomagune.es

1 DOSY experiments

^{1}H NMR and DOSY were performed to study the interaction between DX and PSS in D_2O (Figure S1) and NaCl 500 mM in D_2O (Figure S2). In every figure each colour represents an independent species (DX: red; PSS: green; PSS-DX complex @ R= 10: gray). PSS-DX complex was prepared by mixing DX (300 uL; 8 mM) and PSS (300 µL, 80mM in monomers) in 1:10 molar ratio of PSS/DX in D_2O or NaCl 500 mM. In both Figures S1 and S2, the insets show the stacked ^{1}HNMR spectra relevant to DX (4 mM), PSS (40 mM) and PSS-DX @ R= 10.

The absence of sharp signals of DX in ^{1}H NMR spectra confirms that all DX molecules are complexed to PSS. This is also confirmed by DOSY because no free DX signals are detected for the PSS-DX complex. It has to be highlighted that in both D_2O and the NaCl solution the PSS-DX complex diffuses faster than PSS even if it has a higher MW. This can be explained by the shielding of the sulfonate negative charges by complexation with the positively charged DX, which reduces internal repulsion in the molecules and promotes a more coiled conformation for the PSS molecules.

Table S1 shows the diffusion coefficients calculated from DOSY experiments in D_2O and 500 mM NaCl.

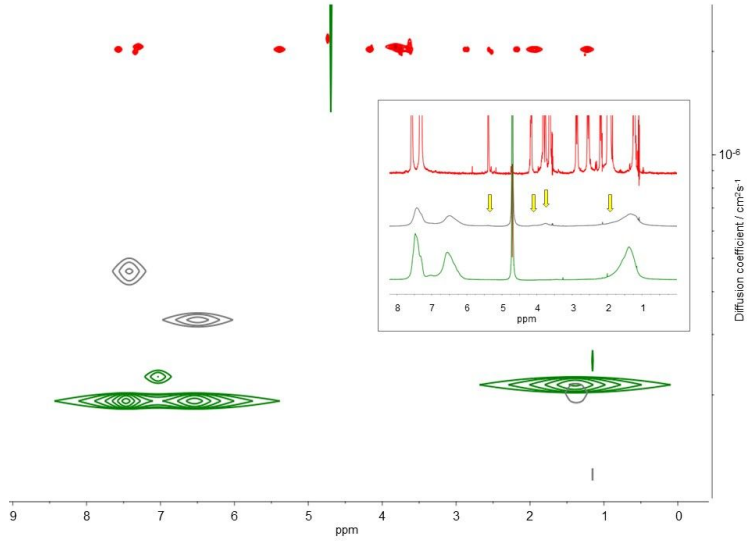

Figure S1: DOSY and ^{1}HNMR (inset) experiments performed on DX (red), PSS (green) and PSS/DX @ R= 10 (grey) in D_2O. Yellow arrows indicate broad DX signals. In all the experiments: $[DX] = 4.0 \cdot 10^{-3}$ M; $[PSS]_{mon} = 4.0 \cdot 10^{-2}$ M.

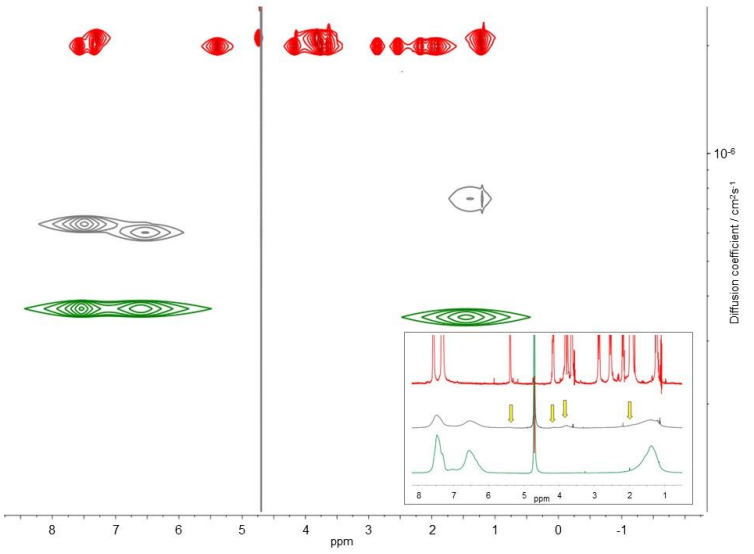

Figure S2: DOSY and ^{1}H NMR (inset) experiments performed on DX (red), PSS (green) and PSS/DX @ R= 10 (grey) in presence of 0.50 M NaCl in D_2O. Yellow arrows indicate broad DX signals. In all the experiments: $[DX] = 4.0 \cdot 10^{-3}$ M; $[PSS]_{mon} = 4.0 \cdot 10^{-2}$ M.

	D (cm^2/s) D_2O	D (cm^2/s) 0.50 M NaCl in D_2O
DX	$2.04 \cdot 10^{-6}$	$2.04 \cdot 10^{-6}$
PSS	$2.03 \cdot 10^{-7}$	$3.66 \cdot 10^{-7}$
PSS/DX @ R=10	$3.25 \cdot 10^{-7}$	$6.63 \cdot 10^{-7}$

Table S1: Self-Diffusion coefficients obtained by the DOSY experiments reported in Figures S1 and S2.

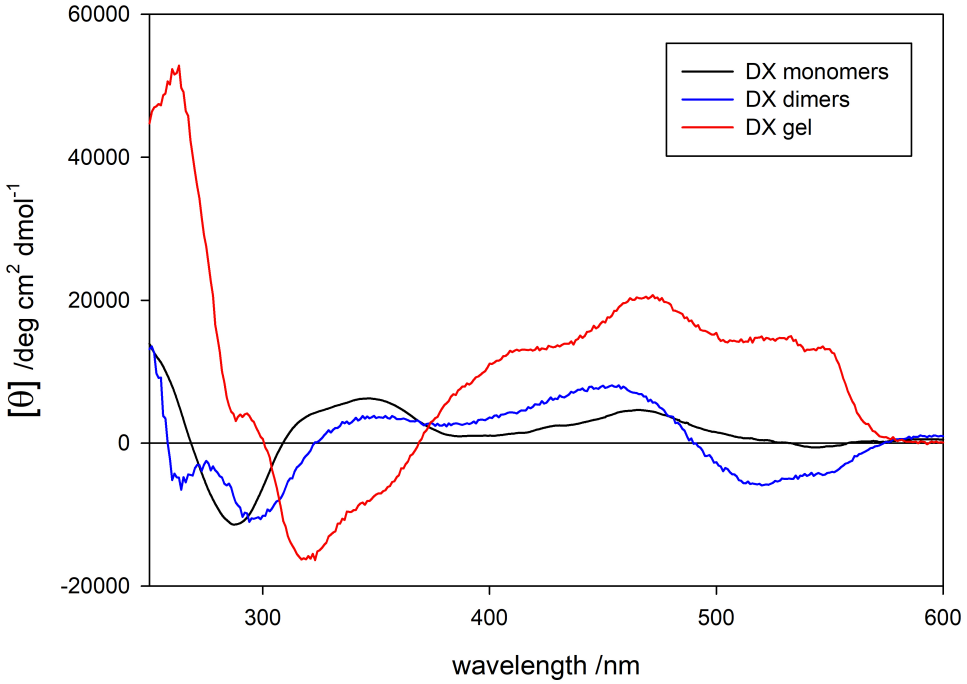

Figure S3: CD spectra of aqueous solutions of DX at T=25 °C. Black: [DX] = $2.3 \cdot 10^{-5}$ M, l=1.00 cm; blue: [DX] = $1.0 \cdot 10^{-2}$ M, l=0.01 cm; red: [DX] = $1.0 \cdot 10^{-2}$ M and [NaCl]=0.75 M, l=0.01 cm.

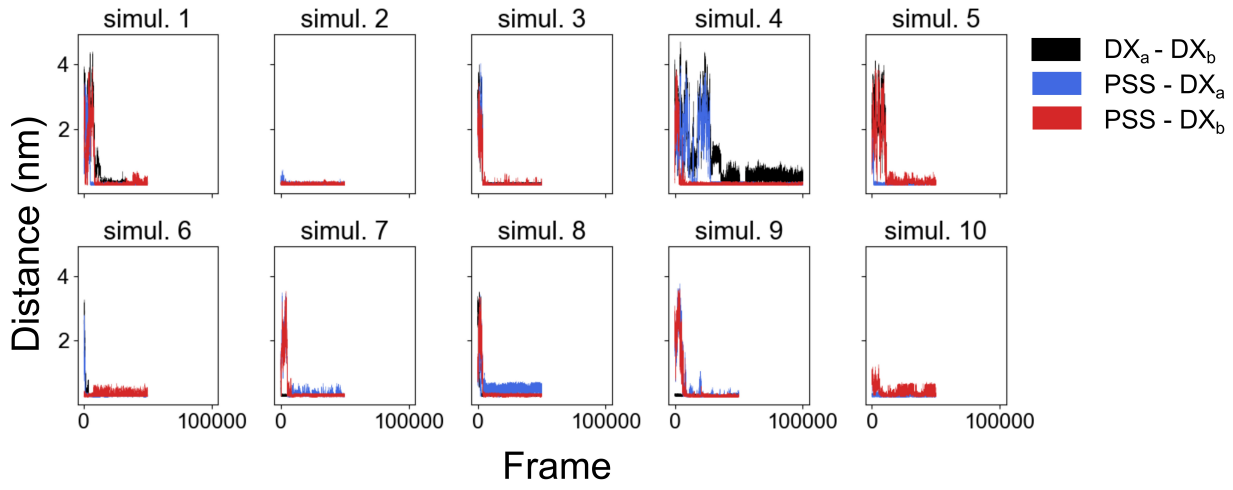

Figure S4: Distribution of the DXa-DXb (black), PSS-DXa (blue) and PSS-DXb (red) minimum distance found among all the pair distances calculated during the 10 MD simulations. Except for the 4-th simulation, which was composed of 10^5 frames, all the others were composed of $5{\cdot}10^4$ frames. The 4-th simulation was carried out up to 10^5 frames since after the first $5{\cdot}10^4$ frames, DXa and DXb and PSS and DXa were still at large distances.

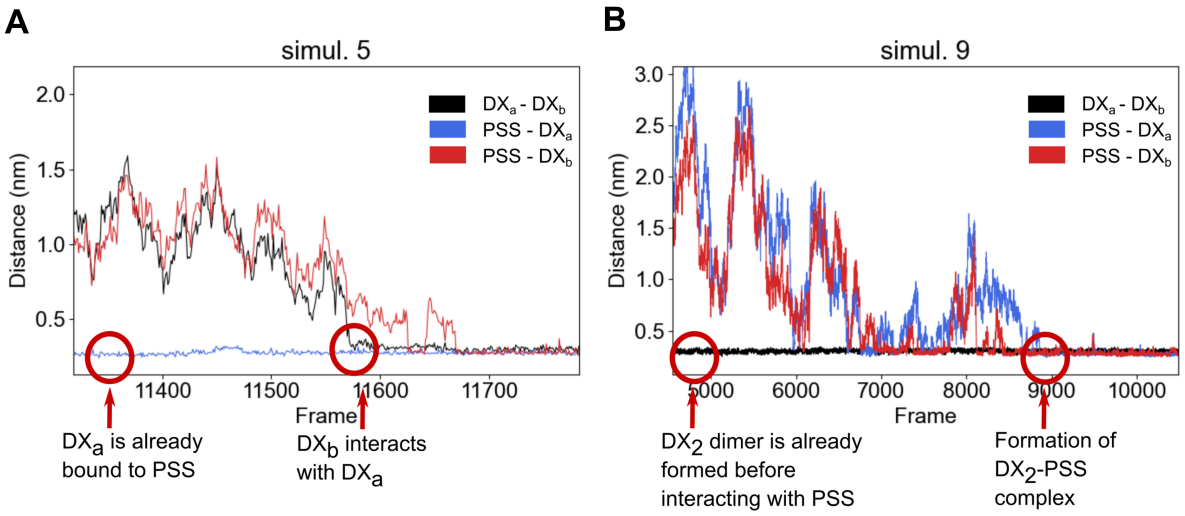

Figure S5: Examples of the information available by MD simulations: the analysis performed on the MD trajectories have been here made explicit for two selected MD simulations (the 5th and the 9th). DXa-DXb (black), PSS-DXa (blue) and PSS-DXb (red) distances during the MD simulations. (A) 5th simulation: DXa forms the DX-PSS complex before interacting with DXb in water. Then DXb interacts with the DX-PSS complex to form the parallel DX dimer bound to PSS (see Fig. 4a in the main text). (B) 9th simulation: the (antiparallel, see Fig. 4b in the main text) DX dimer is already formed before the DX molecules interact with PSS. The DX dimer then binds PSS.

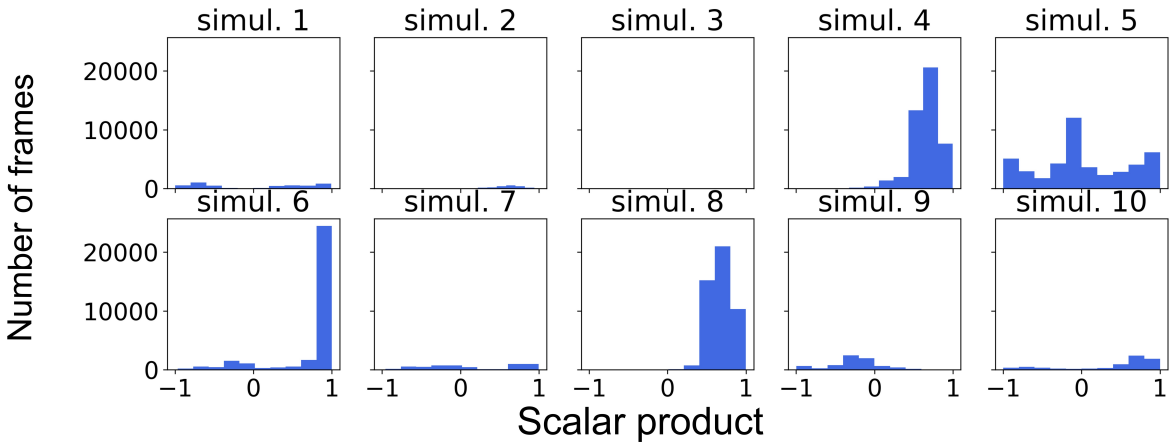

Figure S6: Distribution of the scalar product between the versors describing the two DX molecules as defined in Chart 1 of the main text (-1: antiparallel orientation; 0: orthogonal orientation; 1: parallel orientation) in the 10 additional simulations (starting with one DX already bound to PSS) where such values were observed (each trajectory is composed of a total number of 50000 frames; in each trajectory, only the frames in which the DX dimer was formed and bound to PSS were considered for the calculation of the distribution).

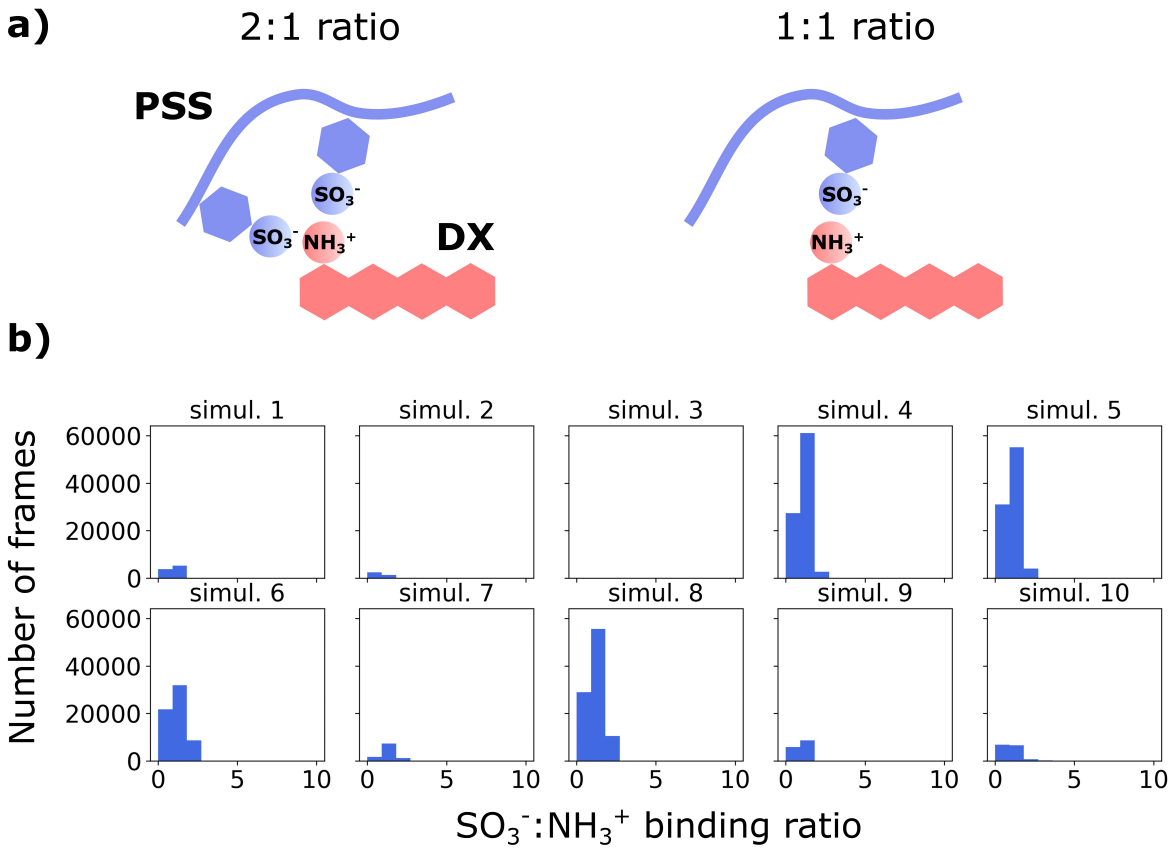

Figure S7: a) Visual representation of the two different conditions in which DX (red) interacts with 1 (right) or 2 (left) sulfonate groups of PSS (blue) b) Distribution of the sulfonate-ammonium binding ratio in the ten additional simulations (starting with one DX already bound to PSS; each trajectory is composed of a total number of 50000 frames; in each trajectory, only the frames in which the DX dimer was formed and bound to PSS were considered for the calculation of the distribution; the same calculation was performed for each DX and finally the distributions were summed; the cutoff distance was set to 0.5 nm, within which the ammonium group of DX and the sulfonate groups of PSS were considered as interacting).

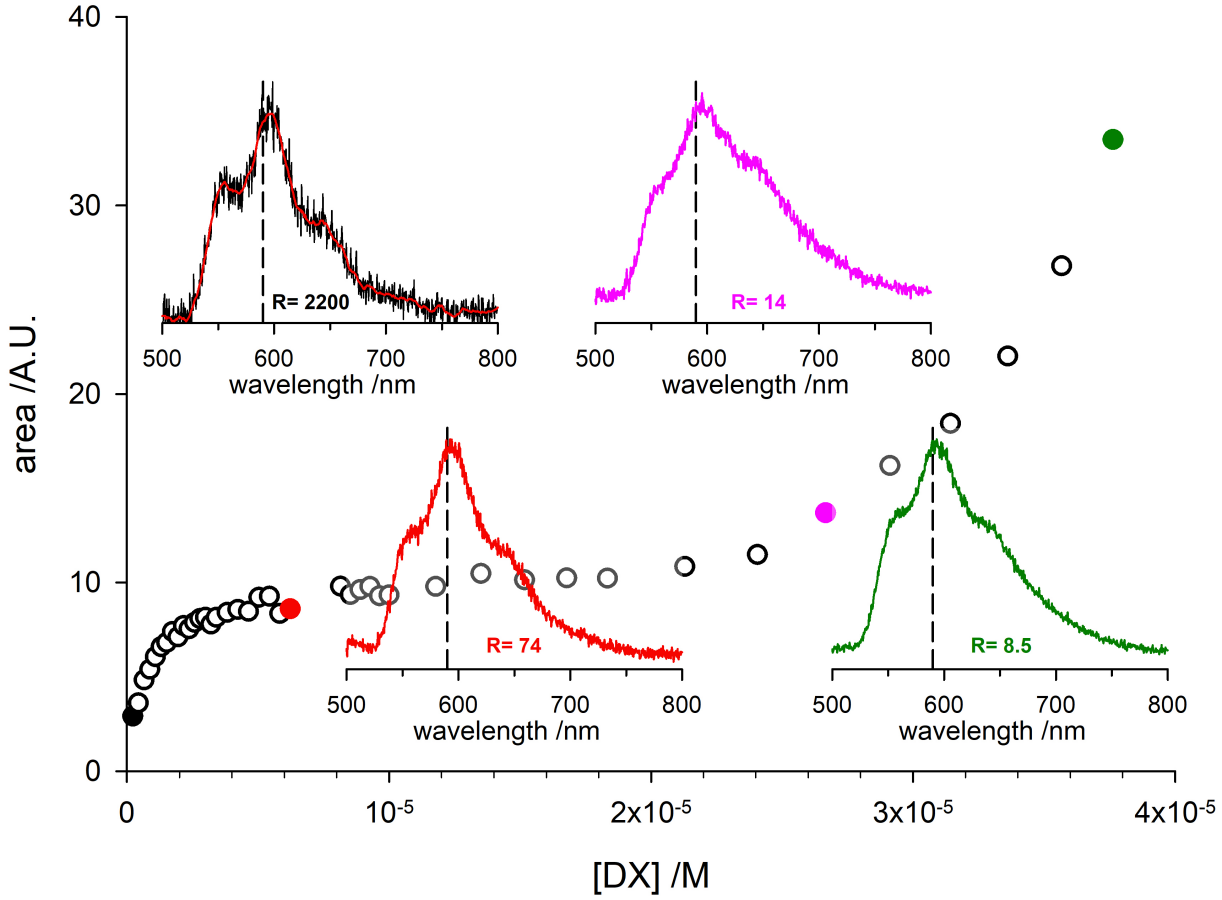

Figure S8: Area of the DX fluorescence spectrum for DX added to a 0.1 mg/mL PSS solution. The insets show a selection of the fluorescence spectra recorded along the titration with the relevant R values (line colour of the spectra matches the corresponding point in the main plot; the dashed vertical line in each spectrum refers to the position of the DX fluorescence emission maximum in water). The increased overall fluorescence intensity on increasing the DX concentration resulted in the increase of the signal to noise ratio of the spectra (the spectrum relevant to the lowest concentration measured - black point in the main graph and black line in the relevant inset - has been smoothed to increase the plot readability - red continuous line).

2 DX-PSS association model

Making reference to the data obtained by the PSS titration with DX (Figure 7 of the main text) performed at the highest PSS concentration explored in this paper (10 mg/mL; green triangles in Figure 7), it is possible to safely assume that the ratio between free DX and DX bound to PSS is in the range of 10^{-5} or even lower and therefore we can consider that the fluorescence measured in these conditions derive from the DX molecules bound to PSS and not quenched since there is a large excess of DX binding sites (R>2000; see Figure 8 of the main text).

The fluorescence intensity (represented by the area of the DX fluorescence spectra) measured at high dilution, where the formation of DX dimers can be safely excluded, allows the calculation of the area of DX bound to PSS when the DX molecules do not quench since they do not interact.

From the linear fit on the area values registered in a 10 mg/mL PSS solution, we found $\hat{A}_{fl} = 2.15 \cdot 10^7 \pm 0.01 \cdot 10^7$, where $\hat{A}_{fl}$ represents the molar fluorescence area of not quenched DX bound to PSS. By comparing this value with that obtained in the case of DX added to water (filled red star symbols in Figure 7 of the main text, $\hat{A}_{fl}^{DX} = 2.40 \cdot 10^7 \pm 0.01 \cdot 10^7$), it is possible to speculate that, for all the DX concentration values explored at 10 mg/mL PSS condition, the extent of quenching due to DX self-association is negligible, as suggested by the linear behaviour of the area measured in the presence of PSS with respect to the same DX concentration intervals in water. The high value of R along this experiment can let us assume that all the DX molecules are bound to PSS, and therefore the $\hat{A}_{fl}$ value can be used to estimate the molar fraction of bound-not-quenched χ_{bnq}, and bound-and-quenched, χ_{bq}, in the 1 mg/mL and 0.1 mg/mL PSS conditions:

$$\chi_{bnq} \cdot \hat{A}_{fl} \cdot [DX] = A_{lowPSS} \tag{1}$$

where A_{lowPSS} is the experimental value of the DX fluorescence signal measured at the PSS concentrations lower than 10 mg/mL (namely, 1 and 0.1 mg/mL).

The χ_{bnq} quantity calculated in the whole DX concentration interval covered by the experiments is reported in Figure S9 as a function of the DX analytical concentration.

It is worth mentioning that in the case of the titration with DX of the 0.1 mg/mL PSS solution, for DX concentrations higher than $1.0 \cdot 10^{-6}$ M (Figure S8 and Figure 7 of the main text), the fluorescence areas remain almost constant when the DX is added to the system. This could be explained by considering that a part of the DX molecules - bound to PSS - can interact with each other, resulting in a quenching of the fluorescence signal. Such a behaviour starts when the ratio (R) between the PSS binding sites and the DX molecules is

R $\simeq$ 100 and it ends at R $\simeq$ 10 (see Figure 8 of the main text). A possible explanation is that within such a R range, the DX molecules can bind to both "free" PSS binding sites as well as to PSS binding sites partially filled by a DX molecule. In the latter case, this may result in the quenching of the "previously fluorescent" DX molecule. This process should lead to a decrease of the fluorescence area, which can be compensated by the fluorescence signal of the DX bound to a "free" PSS binding site. Therefore, the overall effect is to keep the fluorescence area almost constant. At concentration above $6 - 8 \cdot 10^{-5}$ M, corresponding to R $\simeq$ 10 a part of the DX molecules cannot bind to PSS, because almost all the binding sites are filled by DX. This may explain the sharp increase of the area observed at such high [DX] values.

For any given DX analytical concentration, it is therefore possible to estimate the fraction of DX molecules free in solution, bound but not quenched χ_{bnq} and bound and quenched χ_{bq} for any value of the PSS binding sites and that these values are only dependent on R. The results of such calculations leaded to the lines drawn in Figure 8 of the main paper.

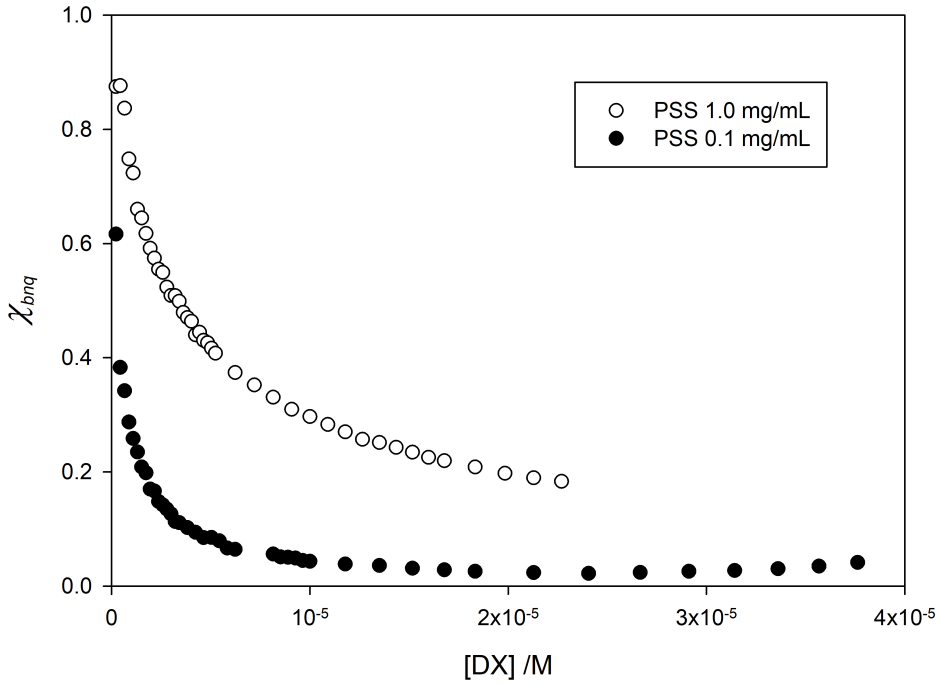

Figure S9: Fraction of unquenched DX molecules bound to PSS (χ_{bnq}) as a function of DX analytical concentration.